Reactions of Pulsed-Laser-Evaporated Thallium Atoms with O_2. Matrix Infrared Spectra of New TlO_2 Species. Trends in Group 13 Dioxides and Dioxide Anions

Lester Andrews,* Gary P. Kushto, and Jason T. Yustein

Department of Chemistry, University of Virginia, Charlottesville, Virginia 22901

Edet Archibong, Richard Sullivan, and Jerzy Leszczynski

Department of Chemistry, Jackson State University, Jackson, Mississippi 39217

Received: July 17, 1997; In Final Form: September 22, 1997[⊗]

Laser-ablated Tl atoms react with O_2 to give a new linear insertion product OTlO and the dimer TlOTlO in addition to the cyclic $Tl(O_2)$, TlO_2Tl, and Tl_4O_2 products observed in earlier thermal effusion experiments. Molecular assignments are based on matrix infrared spectra of oxygen isotopic species. Infrared spectroscopic and quantum chemical evidence is presented for the cyclic molecular anion $Tl(O_2)^-$. Analogous absorptions in Ga and In experiments are assigned to $Ga(O_2)^-$ and $In(O_2)^-$ on the basis of new experiments using a positively biased electrode near the sample and quantum chemical calculations.

Introduction

Recent experiments in these laboratories have shown that laser ablation is an effective means of providing metal atoms as reaction partners for gas-phase and matrix isolation studies. In the case of aluminum, it has been shown that hyperthermal velocities are produced[1,2] and that this extra kinetic energy facilitates reactions that require activation energy.[3] In particular Al insertion into O_2 to give linear OAlO requires activation energy, but addition to give cyclic $Al(O_2)$ proceeds at 25 K. Laser-ablated Ga and In atoms also insert into O_2 to give the linear dioxide molecules,[4] but cold Ga and In atoms only add to give the cyclic species observed in earlier matrix isolation studies with thermal metal atoms.[5,6] In addition a new bent or cyclic species of formula GaO_2 (InO_2) was identified from isotopic spectra.[4] It was decided to explore pulsed-laser-ablated thallium atom reactions with O_2 for the new insertion products in addition to the cyclic TlO_2 species formed by the reaction of thermal atoms.[6,7] In addition, new experiments were performed with a biased electrode near the matrix surface to enhance the trapping of anionic species.

Experimental Section

The apparatus employed for pulsed laser evaporation has been described previously;[8,9] a new Model 22 refrigerator (Cryogenic Technology, Inc.) operated at 10 K. Thallium ingot (Spex, 99.999%) was epoxy glued to a $^1/_4$-20 nut, the front surface was shaved free of oxide layer, and the sample was mounted on a rotatable rod in the vacuum chamber. The laser was operated at 6 Hz in the Q-switched mode with 5−30 mJ/pulse of 1064 nm radiation at the sample. The focused laser pulse produced a green emission from the Tl target. Thallium atoms were co-deposited with $Ar/O_2 = 100/1$ and 200/1 samples for 2−5 h at 2 mmol/h, and infrared spectra were recorded on a Nicolet 5DXB infrared spectrometer from 200 to 4800 cm^{-1} at 2 cm^{-1} resolution. Matrix samples were annealed and/or photolyzed with a 175 W mercury street lamp (Philips H39KB) without the Pyrex globe (240−580 nm).

Complementary experiments were done with a ring electrode positioned on the copper block 3 mm above the cold window using Teflon spacers similar to the electrode employed for electron-impact experiments.[10] Potentials from −125 to +150 V dc were placed on the electrode with the apparatus at ground during sample spray-on, and no discharge was observed. However, the co-deposition of laser-ablated material initiated a discharge on the sample deposition surface. FTIR spectra were recorded on a Nicolet 60 SXR infrared spectrometer using a 6.25 μm Mylar beam splitter and DTGS detector at 0.5 cm^{-1} resolution.

Results

Tl + O_2. Several experiments were done with Tl and O_2 using a range of laser powers, and it was found that 20 mJ/pulse at the sample worked best for these studies. Figure 1a illustrates the spectrum in the 1130−230 cm^{-1} region recorded for this sample co-deposited at 10 K. Ozone, O_4^-, and O_3^- bands were observed at 1039.8, 953.8, and 804.5 cm^{-1} as in previous metal ablation experiments.[3,4,11−14] Note that O_4^- is the strongest product absorption in the deposited sample. New metal reaction product bands were observed at 735.3 cm^{-1} (labeled B following the analogous Ga species),[4] 698.0 cm^{-1} (labeled C), 791.1 cm^{-1} (D), weak 644 cm^{-1} (E), 473.9 cm^{-1} (F), weak 422 cm^{-1} (J), and 1082.3 and 295.2 cm^{-1} (G). The G bands have been identified as cyclic $Tl(O_2)$ and the E bands as Tl_2O by earlier workers.[6,7,15,16] Photolysis with the full light of the medium-pressure mercury arc (Figure 1b) had no effect on the G bands, but increased the B and C band absorbances by a factor of 4 and the F band absorbance by a factor of 2. Photolysis decreased O_3, O_4^-, and O_3^- absorptions as observed previously.[3,4] Temperature cycling from 10 to 15 to 10 K (Figure 1c), where only trapped O atoms can diffuse and react, increased O_3 bands a factor of 3, increased G bands by a factor of 1.2, and increased the F bands a factor of 1.3 without changing the B and C bands. The weak E band increased. A final annealing to 25 K (Figure 1d) markedly increased O_3 and the G bands, slightly increased the D and F bands, decreased the C band by 20%, decreased the 735.3 cm^{-1} B absorption and increased a sharp B satellite absorption at 726.9 cm^{-1}. This annealing also increased the E band, particularly a sharp satellite at 655.9 cm^{-1}, and produced a sharp new E_2 band at 513.2 cm^{-1} and weak G_2 absorptions at 1023.0 and 254.5 cm^{-1}.

[⊗] Abstract published in *Advance ACS Abstracts,* November 15, 1997.

S1089-5639(97)02332-3 CCC: $14.00

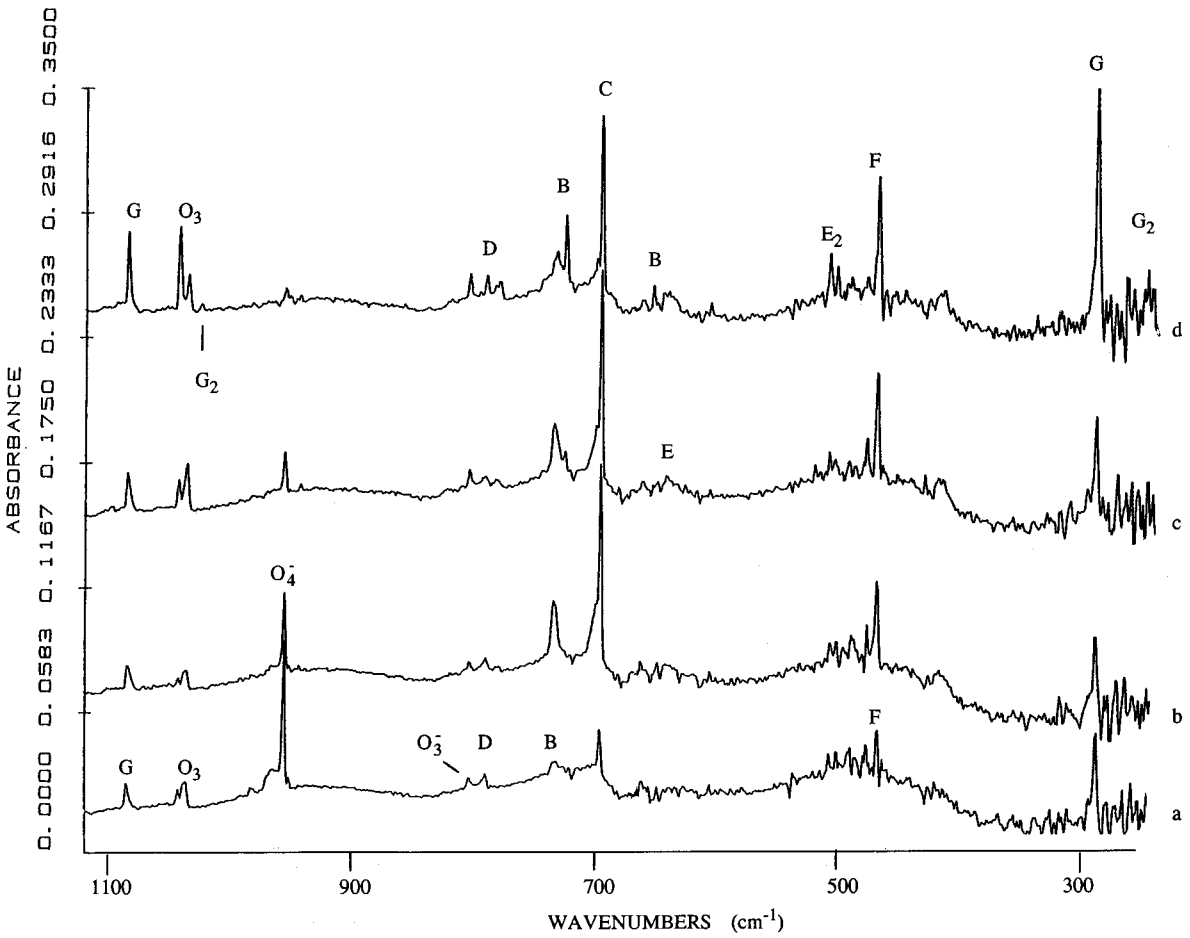

Figure 1. Infrared spectra in 1125−250 cm^{-1} region recorded on Nicolet 5 DXB with 2.0 cm^{-1} resolution for laser-ablated Tl atoms co-deposited with $Ar/O_2 = 100/1$ sample at 10 K: (a) 4 h co-deposit, (b) after broadband photolysis for 30 m, (c) after annealing to 15 K, and (d) after annealing to 25 K.

In other Tl experiments with O_2, the photolysis behavior was even more dramatic. The B, C, and F bands increased by factors of 6−10 on photolysis, and the G bands decreased by 20%. In another experiment with less laser power (about 5 mJ/pulse) the product yield was less. Photolysis with $\lambda > 290$ nm radiation had no effect, but the full light of the medium-pressure arc produced the B, C, and F bands as before. The 735.3 cm^{-1} B band was substantially weaker than the 698.0 cm^{-1} C band, suggesting that species B requires more Tl than species C.

Figure 2 shows the corresponding experiment with Tl and $^{18}O_2$; the same product bands were observed but shifted to lower frequency as listed in Table 1. The B, C, and F bands increased on photolysis (Figure 2b), and the B, D, E_2, and G_2 bands grew on annealing. The F band increased on annealing to 20 K (Figure 2c) and then decreased on annealing to 30 K (Figure 2d).

Two mixed oxygen isotopic experiments were conducted. The first employed mixed $^{16}O_2$ and $^{18}O_2$: the same B, C, E, F, and G bands were observed as described above. Four mixed isotopic ozone bands were observed,[11] as were four D bands at 791.1, 779.4, 758.5, and 747.2 cm^{-1}. The second employed scrambled $^{16}O_2/^{16}O^{18}O/^{18}O_2$: the C, F, and G bands became sharp triplets with intermediate components given in Table 1. Species D revealed five bands, and species B was split into four bands. Figure 3 illustrates the 800−400 cm^{-1} region containing the D, B, C, and E multiplets.

Discharge Deposition Experiments. New experiments were done with indium and oxygen in argon. At lower laser powers the 953.8 cm^{-1} O_4^- band was the strongest product absorption, but at higher laser powers the O_4^- absorption was weaker and bands due to O_3, O_3^-, OInO(C), InO_2'(F), and InO_2(G) were stronger. The approximately 3/1/1 relative absorbance of the three latter bands did not change with laser power and is in reasonable agreement with the earlier laser ablation experiments.[4] Co-deposition of laser-ablated indium with argon and oxygen and from −75 to +150 V dc on the electrode reduced the yield of OInO(C) and increased the yield of InO_2'(F) relative to InO_2(G), giving approximately 1/3/1 absorbance ratios, respectively. The yield of isolated O_3^- at 804.5 cm^{-1} was enhanced 3-fold by the discharge. Positive potentials gave slightly more enhancement than negative potentials.

Three discharge experiments were done with Tl and O_2 using +100 v on the ring electrode, and infrared spectra are shown in Figure 4. Two results were found: (a) on deposition the 473.9 cm^{-1} (E) band was double the 295.2 cm^{-1} (G) band (Figure 4c), whereas the reverse was the case without discharge (Figure 4a), and (b) the 698.0 cm^{-1} (C) band did not increase on photolysis, but on deposition the 698.0 cm^{-1} band was double the 295.2 cm^{-1} band absorbance, which is the relationship found after photolysis without the discharge (Figure 1b). Deposition with threshold laser power and no discharge for 1 h produced the spectrum in Figure 4a; continued deposition for one more hour with identical conditions plus +125 V dc on the electrode gave the spectrum in Figure 4b. Several differences owing to the discharge are noteworthy: (a) the very photosensitive O_4^- species did not increase in yield, (b) the yield of isolated O_3^- increased 5-fold, (c) the F to G band ratio changed favoring species F, and (d) species J (422.5 cm^{-1}) was produced more efficiently with the biased ring. Finally, Figure 4c shows the effect of 2 h deposition with threshold laser power and +100

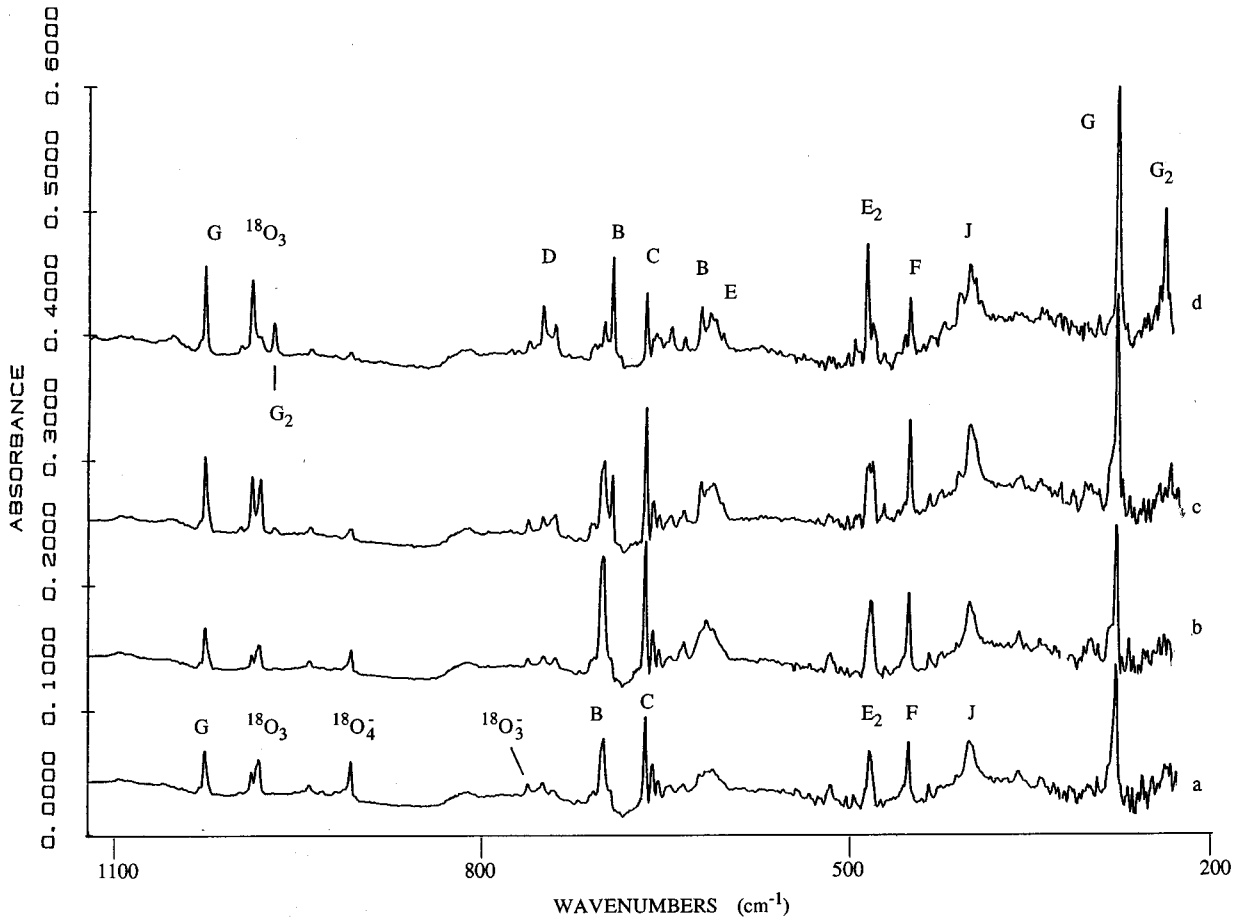

Figure 2. Infrared spectra in 1125−250 cm^{-1} region recorded on Nicolet 5 DXB with 2.0 cm^{-1} resolution for laser-ablated Tl atoms co-deposited with $Ar/^{18}O_2 = 100/1$ sample at 10 K: (a) 4 h co-deposit, (b) after broadband photolysis for 30 m, (c) after annealing to 25 K, and (d) after annealing to 35 K.

TABLE 1: Product Absorptions (cm^{-1}) for Reactions of Pulsed-Laser-Evaporated Tl Atoms with O_2 in Excess Argon

$^{16}O_2$	$^{16}O^{18}O$[a]	$^{18}O_2$	identification
1082.0	1052.6	1021.4	G, cyclic $Tl(O_2)$[b]
1023.0		965.3	G_2, $(TlO_2)_2$[b]
791.1	779.3, 768.2, 758.3	747.5	D, $Tl^+O_3^-$[c]
735.3	725, 715	698.4	B, TlOTlO
726.9	719.5, 705.6	690.7	B, TlOTlO
698.0	684.4	663.8	C, linear OTlO
655.9	643.0, 627.9	619.4	B, TlOTlO
644		610	E, TlOTl[d]
513.2		485.1	E_2, Tl_4O_2[d]
507.3		480.0	E_2 site
473.9	460.3	450.4	F, cyclic $Tl(O_2)^-$
422		402	J, TlO_2Tl[b]
295.2	289.2	280.8	G, cyclic $Tl(O_2)$[b]
254.5		242.2	G_2, $(TlO_2)_2$[b]

[a] New absorptions in $^{16}O_2/^{16}O^{18}O/^{18}O_2$ experiment. [b] Ref 7. [c] Ref 26. [d] Ref 16.

V dc on the surface electrode. The four effects described above are clearly obvious. Applying the voltage *without* laser ablation leads to no discharge on the matrix surface, but laser-ablated material initiates the intense green thallium-seeded discharge glow, which extends back to the thallium target.

Computations

Molecular anions of formula MO_2^- were investigated. The optimized molecular parameters of GaO_2^- were computed at the SCF and MP2 levels using the 6-311+G(2df) basis set. For oxygen, the basis set involves (11s5p) primitives contracted to [6311,311] and augmented with a single set of diffuse Gaussian s- and p-type functions, two sets of d functions, and one set of f functions.[17] For gallium, we employed the recently developed 6-311G basis set of Curtiss et al. supplemented with diffuse and polarizations functions to give the 6-311+G (2df) set.[18] This basis set consists of 128 contracted Gaussian-type functions for GaO_2^-. The calculations for InO_2^- and TlO_2^- were done using Dunning's [4s2p] set on oxygen,[19] and relativistic effective core potentials for In and Tl, with the outer ns^2np^1 (In) and $(n-1)d^{10}ns^2np^1$ (Tl) explicitly treated with the recommended double and triple-ζ basis sets.[20]

Geometry optimizations were carried out at the Hartree−Fock level using analytical gradients. The SCF geometries and force constants were then used to start the optimizations at the second-order Moller−Plesset perturbation (MP2) level. Harmonic vibrational frequencies were obtained from analytic second derivative methods at the SCF and MP2 levels. In the case of InO_2^- and TlO_2^- the force constants were evaluated using numerical methods. At the post-Hartree−Fock levels, the 16 lowest molecular orbitals in GaO_2^- were kept doubly occupied. All calculations were done with the GAUSSIAN 92 program system.[21]

The optimized bond lengths, bond angles, harmonic vibrational frequencies, and infrared intensities are presented in Tables 2−4 for the MO_2^- systems. The frequencies show that both the linear and the cyclic anions are genuine minimum structures on the potential energy surfaces. Examination of the tables also indicates that while in general the linear $(OMO)^-$ anion is the global minimum, the energy difference between the linear and the cyclic $M(O_2)^-$ anions decreases as group 13 is descended from gallium to thallium.

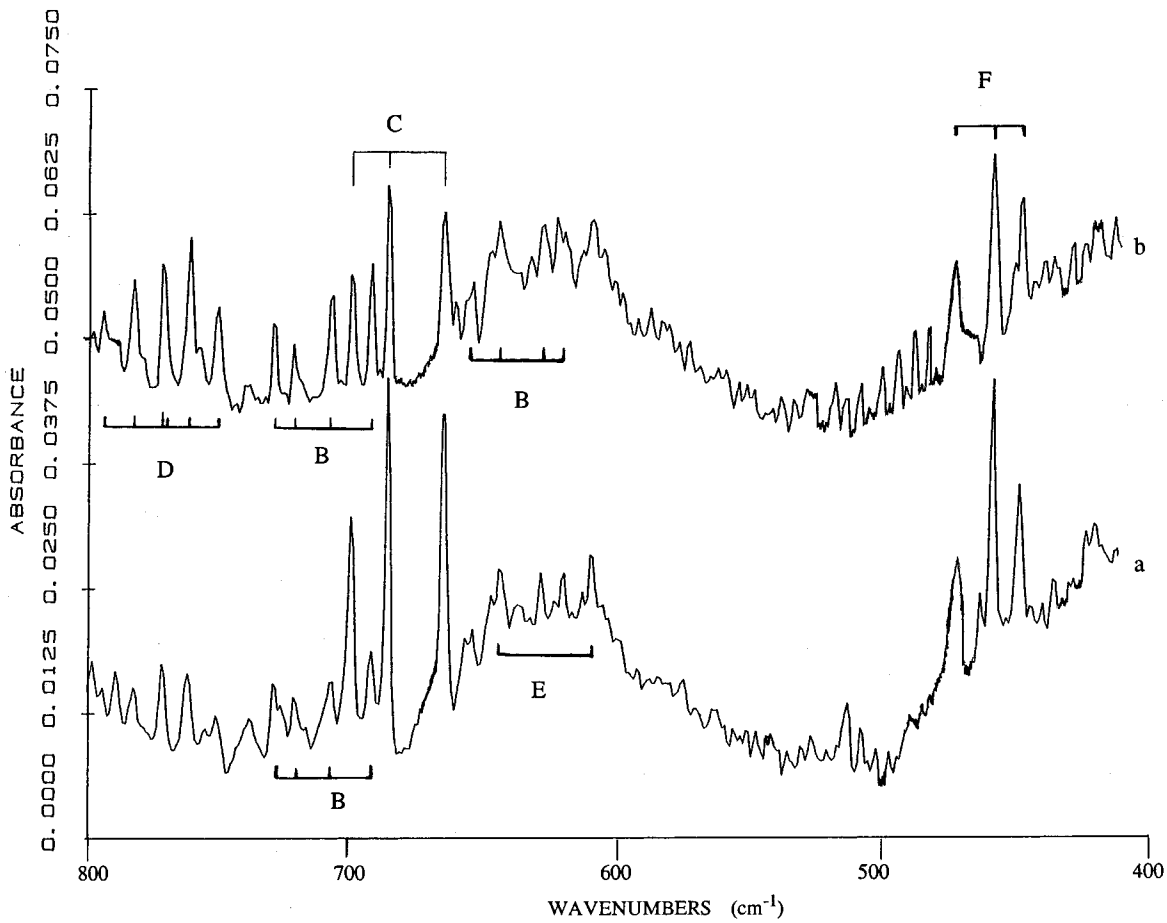

Figure 3. Infrared spectra in the 800−400 cm^{-1} region for laser-ablated Tl atoms co-deposited with $Ar/^{16}O_2/^{16}O^{18}O/^{18}O_2 = 400/1/2/1$ sample for 5 h at 10 K: (a) after photolysis to enhance species c triplet, and (b) after 30 K annealing cycle.

The barrier height corresponding to the conversion of cyclic $Ga(O_2)^-$ to linear $(OGaO)^-$ was obtained by pointwise optimization of the Ga−O bond length. Accordingly, the Ga−O bond distance was optimized for several fixed O−Ga−O bond angles at the MP2/6-311+G(2df) level. A saddle point was found at a Ga−O distance of 2.016 Å and O−Ga−O angle of 67.0° to be 69.8 kcal/mol higher than the cyclic anion form. Thus, electron attachment by the cyclic neutral will form a cyclic anion that is unable to rearrange to the more stable linear anion. Note that the barrier height (3.0 eV) exceeds the EA estimated below (2.0 eV) for cyclic $Ga(O_2)$.

Similar calculations were also done for linear and cyclic BO_2^- and AlO_2^- following the procedure used for GaO_2^-, and these results are summarized in Table 5. Although the linear anions are more stable, the difference decreases markedly for AlO_2^-.

The neutral $Ga(O_2)$ molecule possesses a positive electron affinity (EA), and as the results in Table 6 show, the electron affinity depends very much on the level of theory employed. At the SCF level the adiabatic electron affinity (neglecting the zero-point energy contribution) is 0.9 eV, while at the MP2 level the EA is 2.1 eV. At the CCSD(T) level the EA is estimated to be 1.9 eV. Thus, the electron affinity of the neutral $Ga(O_2)$ may be estimated to be roughly 2.0 eV.

The neutral linear $^2\Pi_g$ OGaO molecule is very difficult to calculate reliably, and the energy at the MP2 level (Ga−O = 1.691 Å) is 6.4 eV above the energy of linear $(O-Ga-O)^-$. This estimate of the electron affinity is probably too high by several eV. The EA of BO has been recently measured[22] as 2.5 eV, and the EA of linear OBO has been reported as 3.8 eV.[23] The EA of linear OGaO is expected to be near the latter value. Accordingly DFT/P3LYP calculations were done with the same basis set, and the anion is found to be lower in energy by 3.8 eV, which is an acceptable estimate for the EA of linear OGaO.[24]

The bonding in cyclic $Ga(O_2)^-$ can be described as $(Ga^+)(O_2)^{2-}$, that is a peroxide type species. This arises because the orbital containing the added electron is the a_2 out-of-plane antibonding π orbital located essentially on the O_2 fragment in the neutral species. The O−O bond distance in $Ga(O_2)^-$ at the MP2 level (1.584 Å) is appropriate for a peroxide species as is the 747 cm^{-1} (O−O) stretching frequency, which is much lower than the superoxide frequency (1092.7 cm^{-1}) observed for neutral $Ga(O_2)$.[5]

Discussion

The thallium oxide product species will be characterized starting with those observed in earlier experiments. A new molecular anion will be identified with the help of new electrode experiments and electronic structure calculations.

Tl_2O and Tl_4O_2. Thallium suboxide, Tl_2O, has been observed at 643 cm^{-1} in solid argon following vaporization of the solid,[15,16,25] and the present weak 644 cm^{-1} band (E) is likewise identified. Annealing increased weak bands at 513 and 507 cm^{-1}, which are close to the strongest band of $(Tl_2O)_2$ at 509 cm^{-1} from the vaporization study[15,16,24] and at 512 cm^{-1} from the reaction of Tl atoms and O_2 using a thermal metal atom source.[7]

$Tl(O_2)$. The strong band at 295.2 cm^{-1} (G) and medium-intensity counterpart at 1082.0 cm^{-1} increased together on annealing and are in excellent agreement with bands observed from the earlier matrix reaction of Tl and O_2. The 295.2 cm^{-1}

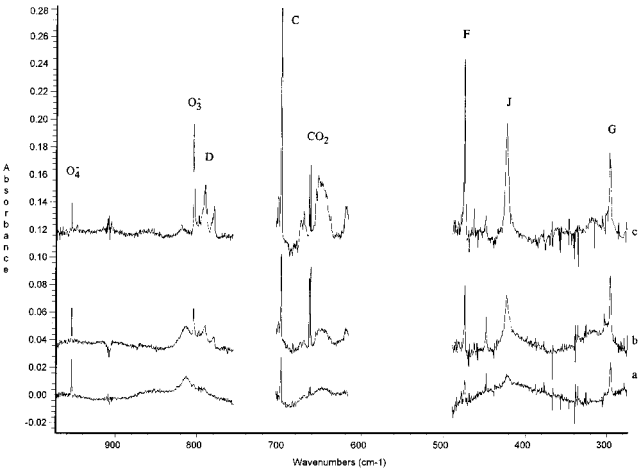

Figure 4. Infrared spectra in the 970−270 cm^{-1} region recorded on Nicolet 60 SXR with 0.5 cm^{-1} resolution for threshold laser-ablated Tl atoms co-deposited with $Ar/O_2 = 200/1$ samples at 10 K: (a) sample co-deposited for 1 h with no electrode voltage, (b) sample co-deposited for 1 more h under identical conditions with +125 V dc on window electrode, and (c) sample co-deposited for 2 h with +100 V dc on window electrode in separate experiment. Spectrum omitted in the 610−490 cm^{-1} region as lack of constructive interference gives only noise and in the 750−705 cm^{-1} region due to detector window absorption.

TABLE 2: Calculated Molecular Properties of GaO_2^- Anions[a]

	SCF/6-311+G(2df)	MP2/6-311+G(2df)
$(OGaO)^-$ ($D_{\infty h}$, $^1\Sigma_g^+$)		
R(Ga−O)	1.669 Å	1.756 Å
absolute energy	−2072.974731 au	−2073.530222 au
zero-point energy	3.36 kcal/mol	3.75 kcal/mol
relative energy	0.0 kcal/mol	0.0 kcal/mol
$^{16}O^{69}Ga^{16}O$	$\sigma_g^+ = 845$ (0)	$\sigma_g^+ = 635$ (0)
	$\pi_u = 253$ (111)	$\pi_u = 493$ (45)
	$\sigma_u^+ = 1001$ (229)	$\sigma_u^+ = 1005$ (880)
$^{18}O^{69}Ga^{18}O$	$\sigma_g^+ = 797$ (0)	$\sigma_g^+ = 599$(0)
	$\pi_u = 244$ (99)	$\pi_u = 474$ (40)
	$\sigma_u^+ = 962$ (207)	$\sigma_u^+ = 966$ (803)
$^{16}O^{69}Ga^{18}O$	$\sigma = 818$ (0)	$\sigma = 616$ (0)
	$\pi = 249$ (105)	$\pi = 483$ (42)
	$\sigma = 984$ (216)	$\sigma = 987$ (841)
$^{16}O^{71}Ga^{16}O$	$\sigma_g^+ = 845$ (0)	$\sigma_g^+ = 635$ (0)
	$\pi_u = 252$ (111)	$\pi_u = 490$ (42)
	$\sigma_u^+ = 996$ (229)	$\sigma_u^+ = 1001$ (847)
$Ga(O_2)^-$ (C_{2v}, $^1A_1$)		
R(Ga−O)	1.861 Å	1.947 Å
θ(OGaO)	47.0°	48.0°
absolute energy	−2072.905918 au	−2073.394770 au
zero-point energy	2.87 kcal/mol	2.51 kcal/mol
relative energy	42.7 kcal/mol	83.7 kcal/mol
$^{69}Ga^{16}O_2$	$a_1 = 958$ (32)	$a_1 = 747$ (17)
	$a_1 = 584$ (176)	$a_1 = 574$ (213)
	$b_2 = 466$ (32)	$b_2 = 434$ (40)
$^{69}Ga^{18}O_2$	$a_1 = 904$ (30)	$a_1 = 704$ (15)
	$a_1 = 561$ (157)	$a_1 = 551$ (193)
	$b_2 = 441$ (28)	$b_2 = 411$ (35)
$^{69}Ga^{16,18}O_2$	$a' = 932$ (31)	$a' = 726$ (16)
	$a' = 573$ (166)	$a' = 563$ (203)
	$a' = 452$ (30)	$a' = 421$ (38)
$^{71}Ga^{16}O_2$	$a_1 = 958$ (32)	$a_1 = 747$ (16)
	$a_1 = 582$ (176)	$a_1 = 571$ (212)
	$b_2 = 465$ (32)	$b_2 = 433$ (40)
$Ga(O_2)^-$ (C_{2v}, $^3B_2$)		
R(Ga−O)	1.894 Å	1.976 Å
θ(OGaO)	95.3°	92.8°
absolute energy	−2072.964374 au	−2073.3478321 au
relative energy	−36.7 kcal/mol	29.5 kcal/mol

[a] Frequencies in cm^{-1}, intensities in km/mol.

band was the strongest absorption after annealing. Isotopic substitution revealed sharp triplet absorption using $^{16}O_2$,$^{16}O^{18}O$,$^{18}O_2$ reagent, which characterizes a species with 2 equivalent oxygen atoms, as observed by Kelsall and Carlson and assigned to the cyclic $Tl(O_2)$ superoxide.[7] The isotopic ratios 1023.0/965.3 = 1.0598 and 295.2/280.8 = 1.0518 define

TABLE 3: Calculated Molecular Properties of InO_2^- Anions[a]

	SCF/ECP+DZ	SCF/ECP+TZ
$(OInO)^-$ ($D_{\infty h}$, $^1\Sigma_g^+$)		
R(In−O)	1.817 Å	1.812 Å
absolute energy	−151.456930 au	−151.460126 au
zero-point energy	2.49 kcal/mol	2.51 kca./mol
relative energy	0.0 kcal/mol	0.0 kcal/mol
$^{16}O^{115}In^{16}O$	$\sigma_g^+ = 674$ (0)	$\sigma_g^+ = 677$ (0)
	$\pi_u = 166$ (114)	$\pi_u = 167$ (116)
	$\sigma_u^+ = 736$ (55)	$\sigma_u^+ = 741$ (60)
$^{18}O^{115}In^{18}O$	$\sigma_g^+ = 635$ (0)	$\sigma_g^+ = 639$ (0)
	$\pi_u = 158$ (101)	$\pi_u = 160$ (104)
	$\sigma_u^+ = 703$ (49)	$\sigma_u^+ = 708$ (53)
$^{16}O^{115}In^{18}O$	$\sigma = 650$ (0)	$\sigma = 654$ (0)
	$\pi = 162$ (107)	$\pi = 164$ (110)
	$\sigma = 724$ (49)	$\sigma = 729$ (54)
$In(O_2)^-$ (C_{2v}, $^1A_1$)		
R(In−O)	2.036 Å	2.023 Å
θ(OInO)	45.0°	45.4°
absolute energy	−151.432449 au	−151.437397 au
zero-point energy	2.46 kcal/mol	2.48 kcal/mol
relative energy	15.3 kcal/mol	14.2 kcal/mol
$^{115}In^{16}O_2$	$a_1 = 872$ (20)	$a_1 = 872$ (19)
	$a_1 = 474$ (99)	$a_1 = 481$ (102)
	$b_2 = 376$ (9)	$b_2 = 385$ (9)
$^{115}In^{18}O_2$	$a_1 = 822$ (18)	$a_1 = 822$ (17)
	$a_1 = 453$ (88)	$a_1 = 459$ (90)
	$b_2 = 356$ (8)	$b_2 = 364$ (8)
$^{115}In^{16,18}O_2$	$a' = 848$ (19)	$a' = 848$ (18)
	$a' = 465$ (93)	$a' = 471$ (96)
	$a' = 365$ (9)	$a' = 373$ (9)

[a] Frequencies in cm^{-1}, intensities in (km/mol).

TABLE 4: Calculated Molecular Properties of TlO_2^- Anions[a]

	SCF/ECP+DZ	SCF/ECP+TZ
$(OTlO)^-$($D_{\infty h}$, $^1\Sigma_g^+$)		
$1\sigma_g^2 1\sigma_u^2 2\sigma_g^2 2\sigma_u^2 1\pi_u^4 1\pi_g^4$		
R(Tl−O)	1.955 Å	1.653 Å
absolute energy	−199.754793 au	−199.756906 au
zero-point energy	2.41 kcal/mol	2.42 kcal/mol
relative energy	0.0 kcal/mol	0.0 kcal/mol
$^{16}O^{205}Tl^{16}O$	$\sigma_g^+ = 648$ (0)	$\sigma_g^+ = 652$ (0)
	$\pi_u = 162$ (76)	$\pi_u = 163$ (77)
	$\sigma_u^+ = 714$ (72)	$\sigma_u^+ = 717$ (78)
$^{18}O^{205}Tl^{18}O$	$\sigma_g^+ = 611$ (0)	$\sigma_g^+ = 615$ (0)
	$\pi_u = 154$ (67)	$\pi_u = 155$ (69)
	$\sigma_u^+ = 679$ (64)	$\sigma_u^+ = 682$ (69)
$^{16}O^{205}Tl^{18}O$	$\sigma = 625$ (0)	$\sigma = 629$ (0)
	$\pi = 158$ (72)	$\pi = 159$ (73)
	$\sigma = 701$ (65)	$\sigma = 704$ (70)
$Tl(O_2)^-$ (C_{2v}, $^1A_1$)		
$1a_1^2 1b_2^2 2a_1^2 1b_1^2 3a_1^2 2b_2^2 1a_2^2 4a_1^2$		
R(Tl−O)	2.221 Å	2.209 Å
θ(OTlO)	40.9°	41.2°
absolute energy	−199.745736 au	−199.749415
zero-point energy	2.34 kcal/mol	2.35 kcal/mol
relative energy	5.65 kcal/mol	4.6 kcal/mol
$^{205}Tl^{16}O_2$	$a_1 = 863$ (46)	$a_1 = 865$ (44)
	$a_1 = 439$ (115)	$a_1 = 443$ (122)
	$b_2 = 335$ (18)	$b_2 = 334$ (20)
$^{205}Tl^{18}O_2$	$a_1 = 814$ (41)	$a_1 = 816$ (39)
	$a_1 = 417$ (102)	$a_1 = 421$ (108)
	$b_2 = 316$ (16)	$b_2 = 315$ (18)
$^{205}Tl^{16,18}O_2$	$a' = 839$ (44)	$a' = 841$ (42)
	$a' = 429$ (108)	$a' = 433$ (115)
	$a' = 325$ (17)	$a' = 324$ (19)

[a] Frequencies in cm^{-1}, intensities in km/mol.

TABLE 5: Calculated Molecular Properties of BO_2^- and AlO_2^- Anions[a]

isotopomers	SCF/ 6-311+G(2df)	MP2/ 6-311+G(2df)
$(OBO)^-$ ($D_{\infty h}$,$^1\Sigma_g^+$)		
$1\sigma_g^2 1\sigma_u^2 2\sigma_g^2 2\sigma_u^2 1\pi_u^4 1\pi_g^4$		
R(B−O)	1.243 Å	1.270 Å
absolute energy	−174.612005 au	−175.179399 au
zero-point energy	6.59 kcal/mol	5.99 kcal/mol
relative energy	0.0 kcal/mol	0.0 kcal/mol
$^{16}O^{11}B^{16}O$	$\sigma_g^+ = 1186$ (0)	$\sigma_g^+ = 1076$ (0)
	$\pi_u = 668$ (92)	$\pi_u = 588$ (38)[b]
	$\sigma_u^+ = 2085$ (904)	$\sigma_u^+ = 1939$ (661)[b]
$^{18}O^{11}B^{18}O$	$\sigma_g^+ = 1118$ (0)	$\sigma_g^+ = 1015$ (0)
	$\pi_u = 659$ (85)	$\pi_u = 579$ (34)
	$\sigma_u^+ = 2055$ (864)	$\sigma_u^+ = 1911$ (630)
$^{16}O^{11}B^{18}O$	$\sigma = 1152$ (0)	$\sigma = 1045$ (0)
	$\pi = 663$ (88)	$\pi = 583$ (36)
	$\sigma = 2070$ (884)	$\sigma = 1925$ (646)
$^{16}O^{10}B^{16}O$	$\sigma_g^+ = 1186$ (0)	$\sigma_g^+ = 1076$ (0)
	$\pi_u = 693$ (95)	$\pi_u = 609$ (38)
	$\sigma_u^+ = 2160$ (958)	$\sigma_u^+ = 2009$ (699)
$^{18}O^{10}B^{18}O$	$\sigma_g^+ = 1118$ (0)	$\sigma_g^+ = 1015$ (0)
	$\pi_u = 683$ (88)	$\pi_u = 601$ (38)
	$\sigma_u^+ = 2132$ (918)	$\sigma_u^+ = 1982$ (669)
$^{16}O^{10}B^{18}O$	$\sigma = 1152$ (0)	$\sigma = 1045$(0)
	$\pi = 688$ (92)	$\pi = 605$ (36)
	$\sigma = 2146$ (938)	$\sigma = 1996$ (684)
isotopic ratio		
R(16/18; σ_u^+)	1.0146	1.0147
R(10/11; σ_u^+)	1.0360	1.0361
$B(O_2)^-$ (C_{2v}, $^1A_1$)		
$1a_1^2 1b_2^2 2a_1^2 1b_1^2 2a_1^2 2b_2^2 1a_2^2 3a_1^2$		
R(B−O)	1.243 Å	1.422 Å
θ(OBO)	63.5°	66.6°
absolute energy	−174.359734 au	−174.932405
zero-point energy	4.18 kcal/mol	3.78 kcal/mol
relative energy	156 kcal.mol	153 kcal/mol
$^{11}B^{16}O_2$	$a_1 = 1358$ (232)	$a_1 = 1226$ (152)
	$a_1 = 947$ (29)	$a_1 = 754$ (11)
	$b_2 = 617$ (4)	$b_2 = 662$ (4)
$(OAlO)^-$ ($D_{\infty h}$,$^1\Sigma_g^+$)		
R(Al−O)	1.603 Å	1.653 Å
absolute energy	−391.744923 au	−392.326024 au
zero-point energy	3.96 kcal/mol	3.42 kca./mol
relative energy	0.0 kcal/mol	0.0 kcal/mol
$^{16}O^{27}Al^{16}O$	$\sigma_g^+ = 886$ (0)	$\sigma_g^+ = 769$ (0)
	$\pi_u = 311$ (174)	$\pi_u = 259$ (84)
	$\sigma_u^+ = 1263$ (269)	$\sigma_u^+ = 1107$ (115)
$^{18}O^{27}Al^{18}O$	$\sigma_g^+ = 836$ (0)	$\sigma_g^+ = 725$ (0)
	$\pi_u = 303$ (159)	$\pi_u = 251$ (76)
	$\sigma_u^+ = 1230$ (248)	$\sigma_u^+ = 1079$ (104)
$^{16}O^{27}Al^{18}O$	$\sigma = 860$ (0)	$\sigma = 747$ (0)
	$\pi = 307$ (166)	$\pi = 254$ (80)
	$\sigma = 1248$ (258)	$\sigma = 1094$ (110)
$Al(O_2)^-$ (C_{2v}, $^1A_1$)		
R(Al−O)	1.750 Å	1.796 Å
θ(OAlO)	50.3°	52.3°
absolute energy	−391.652199 au	−392.206833 au
zero-point energy	3.34 kcal/mol	2.90 kcal/mol
relative energy	58 kcal/mol	74.3 kcal/mol
$^{27}Al^{16}O_2$	$a_1 = 996$ (53)	$a_1 = 823$ (67)
	$a_1 = 741$ (157)	$a_1 = 621$ (66)
	$b_2 = 600$ (10)	$b_2 = 582$ (15)

[a] Frequencies in cm^{-1}, intensities in km/mol. [b] Ref 8, argon matrix 587.8 cm^{-1}, 1931.0 cm^{-1}.

symmetric O−O and Tl−O stretching modes and suggest an O−Tl−O apex angle near 35°. The dimer $(TlO_2)_2$ was also observed at 1023.0 and 254.5 cm^{-1} in agreement with the earlier study.[7]

TlO_3. The bands at 791.1 and 780.7 cm^{-1} (D) are near absorptions assigned previously[26] to the $Tl^+O_3^-$ ozonide species. The present observation of an isotopic multiplet with five bands (missing a weak central component) is in accord with the ozonide assignment.[27]

TlOTlO. The B site at 726.9 cm^{-1} which increases on annealing became a quartet at 726.9, 719.5, 705.6, and 690.7 cm^{-1} with scrambled isotopic oxygen, which denotes 2 inequivalent oxygen atoms. The 726.9/690.7 = 1.0524 ratio is in accord with a Tl−O stretching mode, but this ratio is between the limits of a harmonic diatomic, 1.0560, and the linear O−Tl−O antisymmetric stretching mode isotopic ratio, 1.0519. Clearly the mode is a perturbed antisymmetric O−Tl−O stretching mode, and the likely perturbing species is another Tl atom. The sharp 655.9 cm^{-1} band is one-third of the 726.9 cm^{-1} band intensity, and these bands grow in together on annealing. The 655.9 cm^{-1} band also becomes a quartet with scrambled O_2, and the larger 655.9/619.4 = 1.0598 ratio is indicative of oxygen vibrating between two metal atoms. The oxygen stretching mode for a linear Tl−O−Tl subunit exhibits a 1.0583 16/18 ratio. It follows that the 655.9 cm^{-1} band is due to a perturbed linear antisymmetric Tl−O−Tl stretching mode. Accordingly, the 726.9 and 655.9 cm^{-1} bands are assigned to the two Tl−O stretching modes in the presumably linear TlOTlO molecule. Analogous molecules have been reported for the other group 13 elements,[3,4,8] as contrasted in Table 7.

TlO_2Tl. The weak band at 422 cm^{-1} (J) with $^{18}O_2$ counterpart at 402 cm^{-1} is due to the rhombic peroxide species TlO_2-Tl made by adding another Tl atom to TlO_2, as also found for lithium.[7,28] This band was enhanced in the discharge experiments.

OTlO. The sharp C band at 698.0 cm^{-1} is characterized by marked (2−10-fold) growth on broadband photolysis and a sharp triplet with scrambled isotopic oxygen at 698.0, 684.4, 663.8 cm^{-1}. The 698.0 cm^{-1} band is the strongest product absorption after photolysis. Clearly species C contains 2 equivalent oxygen atoms. The 698.0/663.8 = 1.05152 ratio is slightly smaller than the harmonic ratio 1.05193 predicted for the antisymmetric stretching mode of a linear O−Tl−O molecule. The middle 684.4 cm^{-1} 16-Tl-18 component in the triplet is 3.5 cm^{-1} above the median of the 16-Tl-16 and 18-Tl-18 values, which indicates the presence of the forbidden symmetric stretching mode to lower wavenumbers, but these modes couple in the 16-Tl-18 molecule. Unfortunately, this band was too weak to be observed in the 16-Tl-18 molecule.

As calculations for the molecular anions show, the stable linear $(O-Tl-O)^-$ anion is predicted to have a strong infrared absorption near 700 cm^{-1}. This is near the recently observed ν_3 mode (765 cm^{-1}) for the isoelectronic OPbO molecule.[29] It is possible for photolysis to photodetach a less stable anion, such as O_4^-, and electron capture to form a more stable anion, such as $(OTlO)^-$, so the $(OTlO)^-$ assignment for species C cannot be completely ruled out from the present observations. However, the major reasons for rejecting the linear anion identification for species C are the *marked growth* on broadband ultraviolet photolysis, which should photodetach a molecular anion, and the lack of preference for species C in the electrode experiments, which promote the trapping of charged species.

$Tl(O_2)^-$. The sharp 473.9 cm^{-1} (F) band increases slightly on photolysis and on annealing in these experiments. It becomes a 1/2/1 triplet with scrambled O_2, which identifies another 2 equivalent oxygen atom species. The 473.9 cm^{-1} band is believed to be the thallium counterpart of the GaO_2' isotopic doublet at 568.5, 566.1 cm^{-1} and the InO_2' band at 462.4 cm^{-1}. The GaO_2' and InO_2' absorptions were attributed to bent molecules, but perturbed $(X)(GaO_2)$ species could not be ruled out. Another cyclic GaO_2 species with apex angle (41 ± 2°)

TABLE 6: Electron Affinity of $Ga(O_2)$ Calculated Using 6-311+G(2df) Basis Set[a]

	$Ga(O_2)$ (au)	$Ga(O_2)^-$ (au)	electron affinity (kcal/mol)
MP2	−2073.319134	−2073.394779	47.5 (2.1 eV)
CCSD(T)//MP2	−2073.346850	−2073.415762	43.2 (1.9 eV)

[a] Ref 21.

slightly larger than cyclic GaO_2 with apex angle near 34° was also considered.[4]

The 473.9 cm^{-1} band shifts to 450.4 cm^{-1} with $^{18}O_2$ defining a 1.0522 ratio, which is slightly larger than the TlO_2 value (295.2/280.8 = 1.0513) suggesting a larger valence angle for the TlO_2' species if the observed bands are due to symmetric Tl−O_2 stretching modes in a cyclic TlO_2 moiety. In this case, the intermediate 460.3 cm^{-1} component is 1.9 cm^{-1} below the pure isotopic median frequency due to interaction with a higher wavenumber mode.

The possible observation of a TlO_2 molecular anion was suggested by the observation of a strong O_4^- signal at 953.8 cm^{-1} and O_3^- at 804.5 cm^{-1}. In fact the O_4^- absorbance increased in group 13 metal atom−O_2 experiments with increasing atomic mass, and the O_4^- band intensity with Tl has been exceeded in this laboratory only in lithium−oxygen experiments.[3,4,14,30] Clearly electrons are also ablated from the metal target by the focused laser.

We believe that the positive bias on the electrode attracted electrons from the laser plasma to sustain a discharge on the surface of the matrix. The increase in yield of isolated O_3^- under these conditions attests to the preference for trapping molecular anions. The increase in yield of the 473.9 cm^{-1} (F) band with respect to $Tl(O_2)$ (G) with the biased electrode provides further evidence for the identification of species F as $Tl(O_2)^-$. Similar electrode experiments with indium favored the species F band relative to species G and suggests the $In(O_2)^-$ species.

The $GaO_2'$and InO_2' bands are reassigned here to cyclic molecular anions and the present 473.9 cm^{-1} band is assigned to the analogous cyclic TlO_2^- molecular anion based on agreement with the strongest band predicted by SCF calculations for cyclic GaO_2^-, InO_2^-, and TlO_2^-. The strongest absorption for GaO_2^- is the symmetric mode predicted at 584 and 574 cm^{-1}, which is in excellent agreement with the observed 568 cm^{-1} frequency. Notice also that the Ga 69−71 and O 16−18 shifts are predicted by the calculation within experimental error (Table 2). The weaker O−O and antisymmetric GaO_2^- modes were not observed here. Likewise the strongest $In(O_2)^-$ band is predicted at 481 cm^{-1} as compared to the 462 cm^{-1} observed value. For $Tl(O_2)^-$ the strongest band is predicted at 443 cm^{-1}, below the 474 cm^{-1} observed value. Unfortunately, the other fundamentals, calculated to be weaker, were not observed for the $M(O_2)^-$ molecular anions.

Previous studies at the SCF and CI levels using nonempirical pseudopotentials in conjunction with one-particle basis sets of double-ζ plus polarization quality predicted that the ground state of the neutral cyclic MO_2 (M = Ga, In, Tl) is $^2A_2$.[31] The doublet ground state of the neutral GaO_2 may then capture an extra electron to form either a singlet or a triplet state for the GaO_2 anion. The results listed in Table 2 show that the GaO_2 anion has a singlet ground state with adiabatic $^1A_1-^3B_2$ energy splitting of 29.5 kcal/mol at the MP2 level. The valence electronic configuration of the anion (molecular plane is the *yz* plane) is $(1a_1)^2(1b_2)^2(2a_1)^2(1b_1)^2(3a_1)^2(2b_2)^2(1a_2)^2(4a_1)^2$ giving rise to the $^1A_1$ state, while that of the neutral GaO_2 is $(1a_1)^2(1b_2)^2(2a_1)^2(3a_1)^2(1b_1)^2(2b_2)^2(4a_1)^2(1a_2)^1$ giving rise to the $^2A_2$ state. The highest occupied molecular orbital (SOMO in this case) of the latter is the $1a_2$ antibonding π MO, and examination of the orbital reveals that the effect of double occupation will lead to increase in both the O−O bond length and the OGaO bond angle. Consequently, at the MP2 level the O−O bond length and the OGaO angle are larger in the anion by roughly 0.2 Å and 10°, respectively, compared to the corresponding parameters in the neutral cyclic GaO_2 molecule.

TABLE 7: Comparison of Absorptions (cm^{-1}) for Group 13 Metal Oxides[a]

species	Al	Ga	In	Tl
(B) MOMO	1176	967	816	727
(C) OMO	1129	912	755	698
(D) MO_3	853	850	848	791
	800	842		781
(e) MOM	993	822	735	644
(F) $M(O)_2^-$		568	462	473
(G) $M(O_2)$	496	381	332	295

[a] Refs 3−7.

Reaction Mechanisms. As discussed for previous Al, Ga, and In reactions with oxygen, the primary reactions (1) differ in that addition to form cyclic $Tl(O_2)$ proceeds on annealing without significant activation energy, but insertion to form linear OTlO requires activation energy, which is provided by the laser ablation process.[1−4] This is attested by the observation of cyclic $Tl(O_2)$ by Kelsall and Carlson[7] using 800 K thermal Tl atoms without evidence of linear OTlO. In addition photolysis in the 240−290 nm region increased OTlO markedly without affecting $Tl(O_2)$. Like gallium, apparently the $7s(^2S) \leftarrow 6p(^2P)$ excitation[32] is not effective for insertion, but the higher $6d(^2D) \leftarrow 6p(^2P)$ excitation promotes the insertion reaction.

$$Tl + O_2 \rightarrow \text{cyclic } TlO_2 \quad (1a)$$

$$Tl^* + O_2 \rightarrow \text{linear } [OTlO]^* \xrightarrow{\text{argon}} \text{linear OTlO} \quad (1b)$$

Although TlO was not detected, some TlO was probably formed from decomposition of the energized product of reaction 1b. The presence of TlO is required to form the suboxide on annealing, reaction 2, and the ozonide, reaction 3.

$$TlO + Tl \rightarrow TlOTl \quad (2)$$

$$TlO + O_2 \rightarrow TlO_3 \quad (3)$$

The linear TlO dimer is formed by adding Tl to linear OTlO, reaction 4, as the mixed $^{16}O_2/^{18}O_2$ experiment gave no $^{16}O^{18}O$ product. The rhombic dimer is formed by addition of Tl to cyclic TlO_2, reaction 5, and likewise no $^{16}O^{18}O$ product was observed in the $^{16}O_2/^{18}O_2$ experiment. Table 7 compares the oxide species for Al, Ga, In, and Tl.

$$Tl + OTlO \rightarrow TlOTlO \quad (4)$$

$$TlO_2 + Tl \rightarrow TlO_2Tl \quad (5)$$

Anionic species are formed by the capture of electrons produced in the ablation process, and the positively biased electrode attracts more electrons into the matrix from the laser plasma on the target surface. To maintain change neutrality, some Tl^+ cations must also be trapped in the matrix.

$$O_2 + e \rightarrow O_2^- \quad (6a)$$

$$O_2 + O_2^- \rightarrow O_4^- \quad (6b)$$

$$O_2^- + O \text{ and } O_2 + O^- \rightarrow O_3^- \quad (7)$$

The dominant metal oxide product is probably cyclic $Tl(O_2)$, and electron capture by $Tl(O_2)$ is expected to be an exothermic process based on the electron affinity calculated here for cyclic $Ga(O_2)$, namely 2.0 eV. Rearrangement to the more stable $(OTlO)^-$ linear form is expected to be precluded by a barrier, calculated here to be 3.0 eV for $Ga(O_2)^-$.

$$\text{cyclic } TlO_2 + e \rightarrow \text{cyclic } Tl(O_2)^- \quad (8)$$

Although the linear anion $(OTlO)^-$ is calculated to be slightly more stable, we have no spectroscopic evidence for the linear anion. This could be due to masking by other bands in the 700 cm^{-1} region or to a lower yield of linear OTlO as a precursor for electron capture.

Finally, the $Tl(O_2)Tl$ species was enhanced in the electrode experiments along with $Tl(O_2)^-$. This suggests an additional mechanism for the formation of $Tl(O_2)Tl$, from reaction 9.

$$Tl(O_2)^- + Tl^+ \rightarrow Tl(O_2)Tl \quad (9)$$

The growth of $Tl(O_2)^-$ at the expense of O_4^- on broadband photolysis suggests that electrons photodetached from O_4^- are captured by $Tl(O_2)$. The growth of $Tl(O_2)^-$ on annealing is most likely due to the anion analogue of reaction 1a.

$$Tl + O_2^- \rightarrow Tl(O_2)^-$$

The observation of molecular anions is common in pulsed-laser ablated metal atom reactions with O_2 where O_4^- can be readily observed.[3,4,8] Isolated O_4^- was especially strong in experiments with lithium.[14] In the case of BO_2, the linear $(OBO)^-$ anion was observed, and the ν_3 fundamental of $(OBO)^-$ was 10% as strong as the ν_3 band for OBO.[8] No evidence was found for aluminum oxide anions, but cyclic $Ga(O_2)^-$ and $In(O_2)^-$ anions were observed (present reassignment of GaO_2' and InO_2' species[4]) analogous to cyclic $Tl(O_2)^-$.

It is interesting to note the increase in stability of the cyclic $M(O_2)^-$ species with respect to the linear $(OMO)^-$ species on going from B to Tl in Group 13.

Acknowledgment. We gratefully acknowledge support for this work from National Science Foundation Grants OSR-94-52857 and CHE-97-00116 and assistance with early Tl experiments from P. Hassanzadeh.

References and Notes

(1) Kasatani, K.; Higashide, H.; Shinohara, H.; Sato, H. *Chem. Phys. Lett.* **1990**, *174*, 71.
(2) Salzberg, A. P.; Santiago, D. I.; Asmar, F.; Sandoval, D. N.; Weiner, B. R. *Chem. Phys. Lett.* **1991**, *180*, 161. Wang, H.; Salzberg, A. P.; Weiner, B. R. *Appl. Phys. Lett.* **1991**, *59*, 935.
(3) Andrews, L.; Burkholder, T. R.; Yustein, J. *J. Phys. Chem.* **1992**, *96*, 10182.
(4) Burkholder, T. R.; Yustein, J. T.; Andrews, L. *J. Phys. Chem.* **1992**, *96*, 10189.
(5) Zehe, M. J.; Lynch, D. A., Jr.; Kelsall, B. J.; Carlson, K. D. *J. Phys. Chem.* **1979**, *83*, 656.
(6) Serebrennikov, L. V.; Osin, S. B.; Maltsev, A. A. *J. Mol. Struct.* **1982**, *81*, 25.
(7) Kelsall, B. J.; Carlson, K. D. *J. Phys. Chem.* **1980**, *84*, 951.
(8) Burkholder, T. R.; Andrews, L. *J. Chem. Phys.* **1991**, *95*, 8697.
(9) Hassanzadeh, P.; Andrews, L. *J. Phys. Chem.* **1992**, *96*, 9182.
(10) Suzer, S.; Andrews, L. *J. Chem. Phys.* **1988**, *88*, 916.
(11) Andrews, L.; Spiker, R. C., Jr. *J. Phys. Chem.* **1972**, *796*, 3208.
(12) Andrews, L.. *J. Chem. Phys.* **1971**, *54*, 4935. Thompson, W. E.; Jacox, M. E. *J. Chem. Phys.* **1989**, *91*, 3826. Hacaloglu, J.; Andrews, L., unpublished results.
(13) Andrews, L.; Ault, B. S.; Grzybowski, J. M.; Allen, R. O. *J. Chem. Phys.* **1975**, *62*, 2461.
(14) Andrews, L.; Saffell, W.; Yustein, J. T. *Chem. Phys.* **1994**, *189*, 343.
(15) Brom, J. M., Jr.; DeVore, T.; Franzen, H. F. *J. Chem. Phys.* **1971**, *54*, 2742.
(16) Makowiecki, D. M.; Lynch, D. A., Jr.; Carlson, K. D. *J. Phys. Chem.* **1971**, *75*, 1963.
(17) Frisch, M. J.; Pople, J. A.; Binkley, J. *J. Chem. Phys.* **1984**, *80*, 3265.
(18) Curtiss, L. A.; McGrath, M. P.; Blaudeau, J. P.; Davis, N. E.; Binning, R. C.; Radom, L. *J. Chem. Phys.* **1995**, *103*, 6104.
(19) Dunning, T. H., Jr. *J. Chem. Phys.* **1977**, *66*, 1382.
(20) Hay, P. J.; Wadt, W. R. *J. Chem. Phys.* **1985**, *82*, 270.
(21) Frisch, M. J.; Trucks, G. W.; Head-Gordon, M.; Gill, P. M. W.; Wong, M. W.; Foresman, J. B.; Johnson, B. G.; Schlegel, H. B.; Robb, M. A.; Replogle, E. S.; Gomperts, R.; Andrew, J. L.; Raghavachari, K.; Binkley, J. S.; Gonzalez, C.; Martin, R. L.; Fox, D. J.; Defrees, B. J.; Stewart, J. J. P.; Pople, J. A. *GAUSSIAN 92/DFT*; Gaussian, Inc.: Pittsburgh, PA, 1992.
(22) Wenthold, P. G.; Kim, J. B.; Jones, K.-L.; Lineberger, W. C. *J. Phys. Chem. Ac.* **1997**, *101*, 4472.
(23) Srivastava, R. D.; Uy, O. M.; Farber, M. *Trans. Faraday Soc.* **1971**, *67*, 2941.
(24) Using the Gaussian 94 program system, DFT/B3LYP calculated parameters for $(OGaO)^-$ are Ga−O = 1.695 Å, frequencies (intensities) are 919 cm^{-1} (193 km/mol), 765 cm^{-1} (0 km/mol), 215 cm^{-1} (2 × 59 km/mol) and for (OGaO) are Ga−O = 1.696 Å, 662 cm^{-1} (736 km/mol), 754 cm^{-1} (0 km/mol) and 186, 201 cm^{-1} (42, 41 km/mol).
(25) Hinchcliffe, A. J.; Ogden, J. S. *J. Phys. Chem.* **1971**, *75*, 3908; **1973**, *77*, 2537.
(26) Sonchik, S. M.; Andrews, L.; Carlson, K. D. *J. Phys. Chem.* **1984**, *88*, 5269.
(27) Spiker, R. C., Jr.; Andrews, L. *J. Chem. Phys.* **1973**, *59*, 1851.
(28) Andrews, L. *J. Chem. Phys.* **1969**, *50*, 4288.
(29) Chertihin, G. V.; Andrews, L. *J. Chem. Phys.* **1996**, *105*, 2561.
(30) Andrews, L.; Yustein, J. T.; Thompson, C. A.; Hunt, R. D. *J. Phys. Chem.* **1994**, *98*, 6514.
(31) Cabot, P. L.; Illas, F.; Ricart, J. M.; Rubio, J. *J. Phys. Chem.* **1986**, *90*, 30.
(32) Mitchenko, N., S.; Predtechenskii, Yu. B.; Shcherba, L. D. *Opt. Spectrosc.* **1976**, *41*, 521.